

Experiments on Reduction in Drag of Circular Cylinder at Transonic Speed by Using Wire

Mochamad Dady Ma'mun

Email: dadymamun@yahoo.com

Department of Aerospace Engineering, Nurtanio Bandung University,

The effects of small diameter of wires on reducing drag of flow around a circular cylinder at transonic speeds were examined experimentally. The wires were attached longitudinally at an asymmetrical location with regard to the symmetry plane and acted as a barrier restricted upstream propagation of instabilities originate in the downstream wake. The experiment was investigated at Mach numbers of 0.6 and 0.73 and the flow was considered laminar boundary layer on the cylinder surface. The results clearly showed that depending on the Mach number, the wires effectively reduced the pressure drag by 13.2% for Mach number 0.6 and 4.4% for Mach number 0.73, respectively. Assuming the existence of shock waves that produced so-called wave drag, the wires also reduced the total drag: by 14% for Mach number 0.6 and 6% for Mach number 0.73..

Key words: pressure drag, wave drag and transonic speed.

1. Introduction

The flow past a circular cylinder is considered as a model problem to understand the flow in the wake of a bluff body. The main feature of the flow past a bluff body is its separation from the body surface happened ahead of the rear stagnation point, which causes the formation of a periodic vortex pattern known as the Karman vortex street. The presence of the vortical wake alters the flow and the pressure distribution on the body surface given by the potential flow solution, which results in a pressure deficit on

the after body surface and an excess in the upstream pressure. Consequently, the real drag is quite distinct from that provided by the potential flow theory. A continuing struggle for the practicing aerodynamics is that to minimize this drag; any reduction of the drag leads to either fuel savings or performance, improvements.

Besides yielding high drag, it has been shown that the flow oscillations induced by the Karman vortex street around a cylinder are considerably high and cannot be treated simply as small perturbations superimposed

on the undisturbed flow especially in transonic flows¹⁾. Therefore, it is very challenging and of great practical importance for engineering applications to control the Karman vortex street in the wake region.

This phenomena has been of interest of researchers for decades. Many attempts have been made for controlling the wake behind a cylinder, especially for the purpose of suppressing the formation of the Karman vortex street by using passive or active controls. However, the explanation of the mechanism that leads to the formation of this vortex is not well understood to the present.

What seems to be appreciated by researchers is that the development of the vortex street is caused by the interaction of separated shear layers shedding from upper and lower surfaces of the cylinder. This interaction was demonstrated by Roshko²⁾ by inserting a plate along the plane of symmetry to divide the two shear layers. The presence of the plate greatly influences the development of the vortex pattern, resulting in a lower Strouhal number and a higher base pressure.

Roshko^{1,9)} made also an important observation that the base pressure distribution plays a certain

role in the process of the vortex formation. He proposed the following relation for the base pressure

$$Cp_b = 1 - k^2 \quad (1)$$

with

$$k = \frac{U_s}{U_\infty}$$

where U_s is the velocity at the separation point and U_∞ is the free stream velocity.

Moreover, he suggested a relation for the Strouhal numbers, which can be written as

$$S = \frac{d}{l} \left(1 - \frac{U}{U_\infty} \right) \quad (2)$$

where d is the diameter of the cylinder, l is the distance between two consecutive vortices and U is the velocity of vortex motion relative to the free stream flow. The vortex velocity and the flow velocity at the separation point are related by

$$\frac{U}{U_\infty} = \frac{1}{2} \left(1 - \sqrt{1 - \frac{\varepsilon k^2}{\sqrt{2}}} \right) \quad (3)$$

where ε is the fraction of the shear layer vorticity that captured by an elemental vortex in the Karman vortex street. By using these relations he determined that $S = 0.206$, which well agrees with the

experimentally observed value in incompressible flows.

To control the base pressure distribution, Bearman³⁾ investigated the flow behind a two dimensional model with a blunt trailing edge and fitted with splitter plates. He measured the base pressure and the frequency shedding of vortices and showed that the existence of splitter plates, significantly being increases the base pressure and the vortex formation length L_f and that base suction is inversely proportional to this length:

$$-Cp_b \propto \frac{1}{L_f} \quad (4)$$

Many researchers have obtained certain advantages in controlling the vortex-street in low-speed applications. However, transonic flow regimes have not sufficiently investigated, and the control of vortical wake flow is still a challenging problems.

2. Experimental setup and procedure

The experiment was conducted in the transonic wind tunnel of Fluid Dynamics Laboratory, Aerospace Engineering Department, Nagoya University Japan. The wind tunnel was of an induction type and operated at atmospheric total

pressure and temperature. The schematic drawing of the tunnel was given in Figure 1. The tunnel was built vertically and had a closed-loop structure. The test section was a rectangular with 30 cm wide and 40 cm high cross sectional area. The top and bottom walls of the test section were ventilated with fixed geometry longitudinal slots, which had compromising 7% open area. The tunnel used high-pressure air, which was stored in a 12m³ reservoir with a maximum pressure capacity of 40 kg/cm². The two-dimensional models could be mounted on side walls. Three-dimensional models were implemented by a circular-arc sting support.

The tunnel was an atmospheric facility, and in principle, Mach numbers could be achieved between 0.4 and 1.2 in the test section. To get required Mach numbers, a flap was used, which was located almost immediately behind the test section, as shown in figure.2. The tunnel was driven by injecting high-pressure air through the injector, which induces the flow of air in the test section. The injected air was released to the atmosphere through an air vent located in the low-speed leg of the circuit. Atmospheric air was drawn into the tunnel through the same vent to maintain the flow condition in

the test section at the atmospheric level. Flow control was realized manually by adjusting the supply of

air into the tunnel through the pneumatic valve.

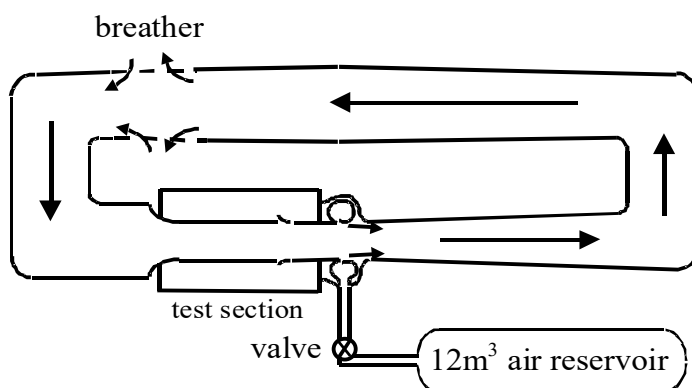


Figure 1. Schematic of wind tunnel

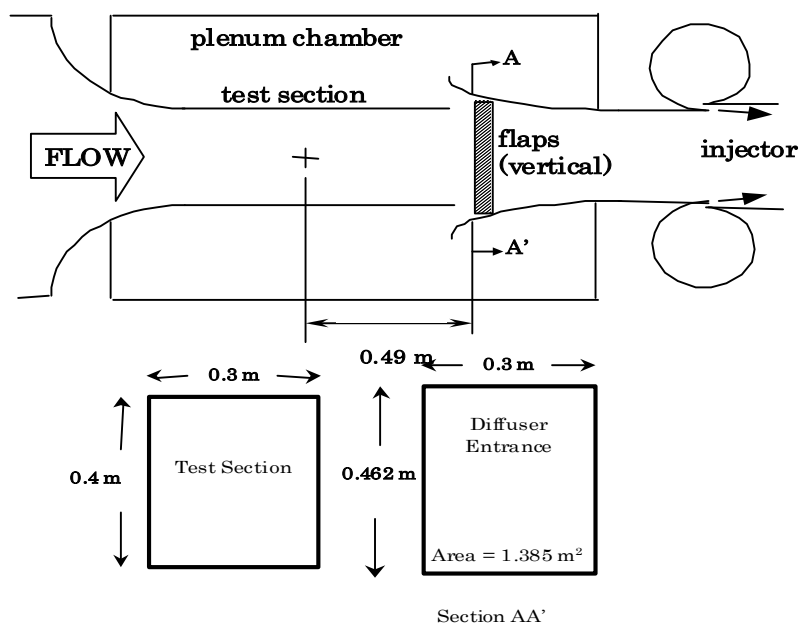


Figure 2. Schematic of wind tunnel test section

The cylinder model was made from aluminum. It has a diameter of 30 mm and a length of 300 mm. The schematic drawing of the model was given in figure 3. This cylinder was

span wise installed between two side walls. The cylinder can be rotated around its longitudinal axis that allowed us to measure the circumference pressure distribution

on the cylinder surface.

Seven pressure taps were uniformly distributed along the surface of the cylinder from the leading edge to the trailing edge with a step $\Delta\theta$ of 30° intervals, where θ was the angle measured from the leading edge to the trailing edge. By rotating the cylinder, pressure data on the surface of the cylinder can be

measured at 10-degree intervals.

Besides the basic smooth cylinder, the wire cylinder was also tested. Wires were made of stainless, have the diameter $d=1.5$ mm and length of 300 mm. The wires were span wise attached to the rear region of the cylinder at different locations.

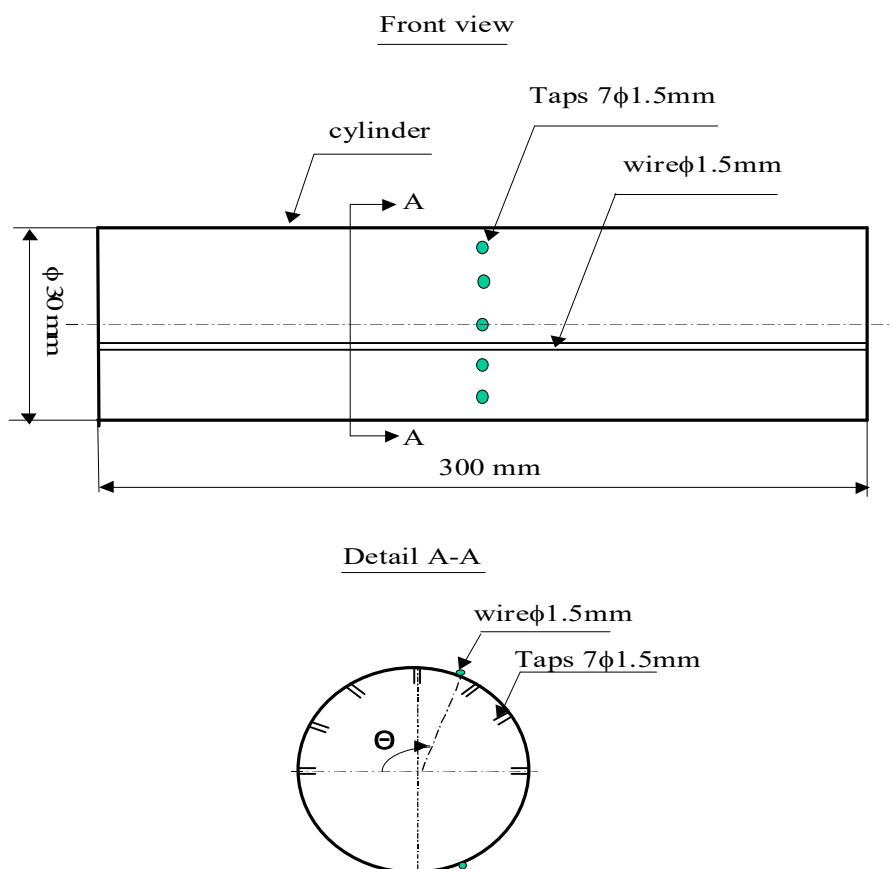


Figure 3. Schematic of experiment model

The experiment had been conducted at two Mach numbers, i.e. $M = 0.6$ and $M = 0.73$, which corresponds to a Reynolds number based on the cylinder diameter of

4.0×10^5 and 4.8×10^5 , respectively. Under these conditions the boundary layer on the cylinder surface was expected to be laminar. In the case of incompressible flow,

the both values of the Reynolds number are greater than the critical Reynolds number. Therefore the boundary layer was supposed to be in the transitional or turbulent state. However, as the Mach number increases the critical Reynolds number increases as well. Achenbach and Heinecke⁴⁾ compiled data of several investigators, and a data from transonic tunnel showed that at Mach 0.46 the critical Reynolds number is approximately 3×10^6 , i.e. almost one order higher than the Reynolds numbers used in the present experiment. The blockage ratio was about 7.5% of the test section area. A reference pitot-static tube was installed upstream of the cylinder and displaced in the cross flow direction to reduce interference with the flow past the cylinder.

In order to measure the distribution of the total pressure loss behind the cylinder model, a total pressure rake was used. The rake was placed at a distance of four

cylinder diameters behind the cylinder. This location was assumed to be sufficient to cover the whole of the wake. A schematic drawing of the rake is given in figure 4. The strut was made from a commercially available steel pipe and had a span size of 55 cm, a chord length of 4 cm and a thickness 1 cm. 17 steel tubes of 1.5-mm diameter were installed at the leading edge of the strut. The tubes protruded at a distance of 3.5 cm from the strut's leading edge and were allocated with a step of 0.5 cm.

The tubes can be connected to the pressure transducer that was located outside the wind tunnel. Similar to the steady pressure measurements, the signal from each transducer was amplified by using Kyowa DPM-8H amplifier and was then fed to a NEC PC-9821 XS personal computer through a AD12-8RT A/D board. The schematic drawing of the data acquisition system for this case is given in figure 5.

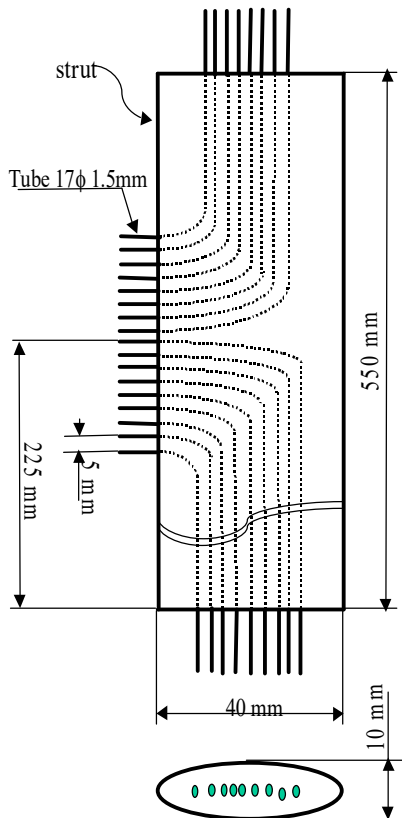


Figure. 4. Schematic of Rake

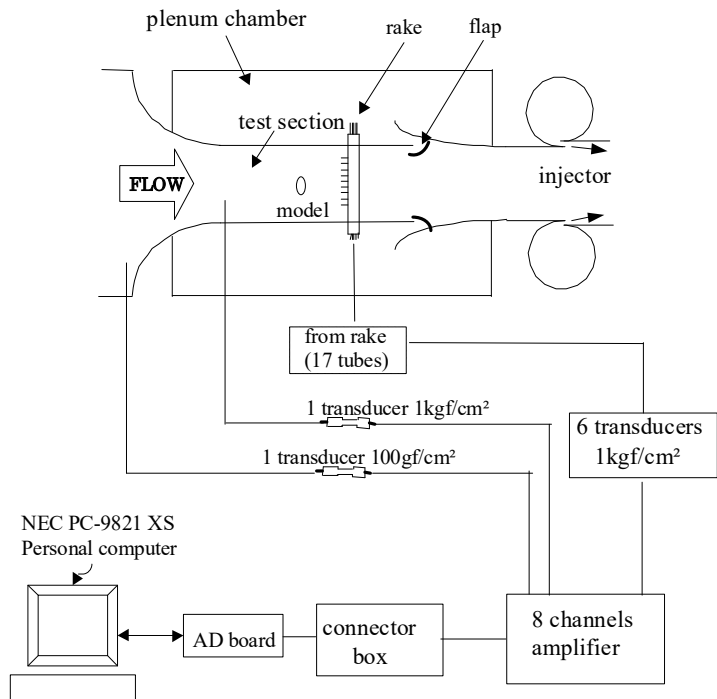


Figure 5. Schematic of pressure measurement system at rake

3. Wires Effect on Pressure Measurement

3.1. Base Pressure

The base pressure considered in the present study was the pressure measured at the rear stagnation point of the cylinder, i.e. at $\theta = 180^\circ$. The effect of wire on the base pressure was displayed in figure 6 where the base pressure coefficient C_{pb} was plotted against the wire position θ_w for both Mach number 0.6 and 0.73.

These figures showed that the maximum of the base pressure was achieved when the wire was located at $\theta_w = 110^\circ$ and $\theta_w = 100^\circ$ for Mach number 0.6 and 0.73, respectively. These also respond to the minimum in the pressure drag as can be seen in section 3.3. As can be seen the maximum base pressure was achieved at different wire locations for Mach numbers 0.73. This can be explained by the presence of the shock wave when Mach number

was 0.73⁶⁾. The existences of the shock wave can prevent the downstream perturbations to propagate upstream and thickening the boundary layer when the shock wave induced them. It caused the free shear layer pattern behind cylinder was different from the case of Mach number 0.6.

Nevertheless, for both Mach numbers the presence of wire leads to an increase in the base pressure.

This can be explained by the decrease in suction, and, as result delaying in the formation of vortex so as the vortex structure was developed more downstream. This result agreed well with the resulted obtained by Bearmen³⁾, who showed that the base pressure was approximately inverse proportional to the distance of the fully vortex formation.

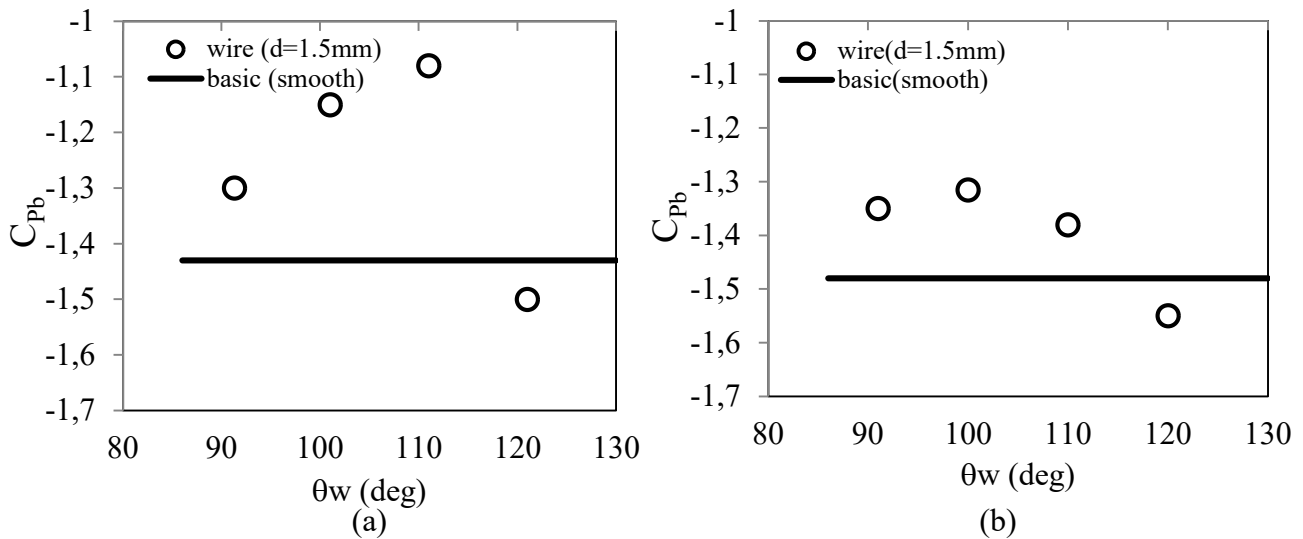


Figure 6. Base pressure distribution with/without wires: (a) Mach number 0.6, (b) Mach number 0.73

For comparison, the base pressure for different wire diameters was also plotted in figure 7 for both Mach number 0.6 and 0.73, respectively. These figures showed that the wire with the diameter 0.6 mm slightly increased the base

pressure. This case was not so effective compared to others. For example, in the case of wire with the diameter 1 mm and 1.5 mm the base pressure was increased much more. Consequently, the pressure drag was reduced.

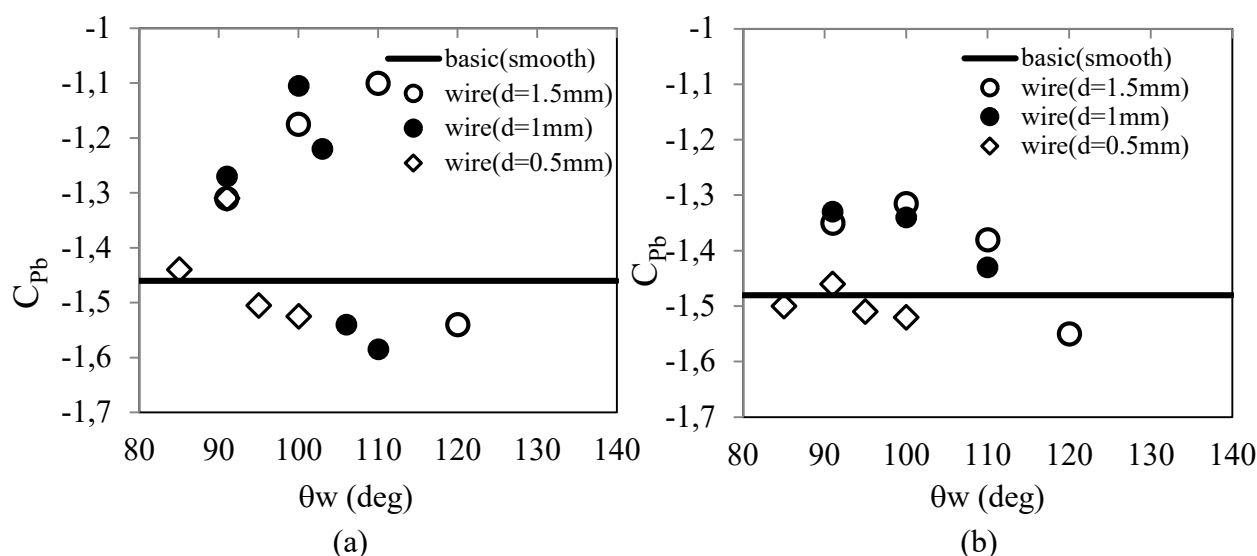


Figure 7. Base pressure distribution with a parameter of wires size:
 (a) Mach number 0.6, (b) Mach number 0.73

3.2. Pressure Distribution

The pressure distribution data obtained on the present study represents the time-averaged pressure taken by the steady pressure measurement. The experiment was done with two **Symmetrical Double-wires**

The time-averaged pressure distribution at Mach number 0.6 for the symmetrical double-wire configuration was shown in figure 8a, where wires were symmetrically installed at $\theta_w = 110^\circ$. The pressure distribution for this configuration, one can see that there was de-coupling of the pressure fields upstream and downstream of the wire. In the upstream the pressure was less compared to the smooth cylinder. However, the flow

configurations of wires i.e. symmetrical double-wire and four-wire. The symmetrical four-wire configuration was done to see the effect of adding wires numbers from symmetrical double-wire downstream of the wire attains much higher pressures.

In other words, there was a pressure jump across the wire. The increasing pressure distribution relates with the change of the pressure gradient, which made the separation point to occur more downstream. The pressure gradient in upstream of separation point for the wire case has more negative value compared to the smooth one.

The time-averaged pressure distribution at Mach number 0.73 for

this configuration was shown in figure 8b, where the wire was also installed at $\theta_w = 110^\circ$. It was seen that similar to the case of Mach number 0.6, the de-coupling of flow fields was also occurred. The pressure in upstream of the wire is slightly lower compared to the smooth cylinder case. At $\theta = 80^\circ$, the shift to the minimum location was clear. This point was predicted as the separation point that coincided with the existence of the strong shock waves for this Mach number

as shown by Tombi L.⁶⁾. In fact, the separation was probably shock induced. As the flow separation was highly unsteady process, the location of the separation point was always changed and cannot be determined from the steady measurement data only. However, the downstream pressure was slightly higher compared to the smooth cylinder, but the increase in the pressure was not so high in the case of Mach number 0.6.

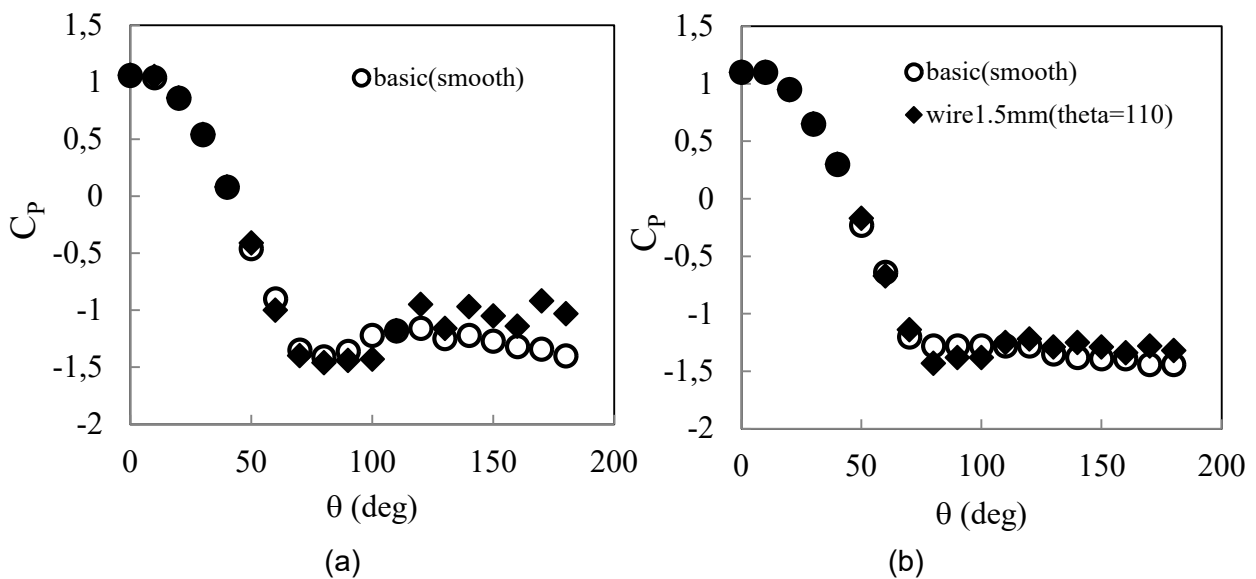


Figure. 8. Effect of symmetrical double-wires on pressure distribution: (a) Mach number 0.6, (b) Mach number 0.73

Symmetrical Four-wires

The four-wire configuration used four wires of the diameter 1.5 mm, which were installed symmetrically at $\theta_w = 110^\circ$ and $\theta_w = 120^\circ$ in tandem. This configuration was tested to see the effect of adding wire on the

pressure characteristics.

The time-average pressure distribution for this configuration was shown in figure 9 for both Mach number 0.6 and 0.73, respectively. For comparison the results of double-wire configuration were also

plotted. These show that the pressure distribution for this configuration has almost no different compared to the case of double-wire configuration. Therefore, the number of wires has no significant effect on the pressure distribution compared

to the case of two wires. The pressure was only slightly increased in comparison with the double-wire configuration. This can influence the pressure drag as can be seen in table 1.

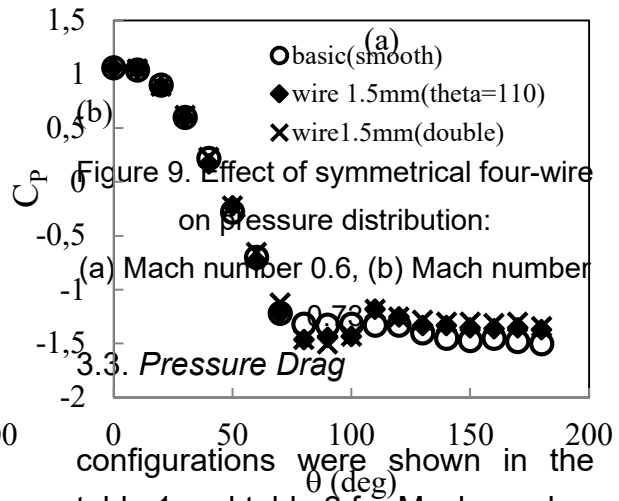
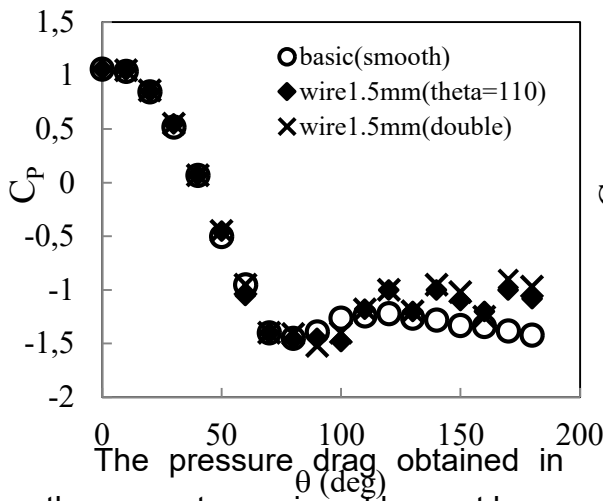


Figure 9. Effect of symmetrical four-wire on pressure distribution:

(a) Mach number 0.6, (b) Mach number 0.73.

3.3. Pressure Drag

The pressure drag obtained in the present experiment has not been directly measured, but was calculated from the results of the pressure distribution. The pressure drag in this calculation using relation followed⁵⁾:

$$C_d = \int_0^{2\pi} C_p \cos \theta d\theta$$

where C_p was the pressure coefficient and θ was the angle from the leading edge (front) to the trailing edge (back)

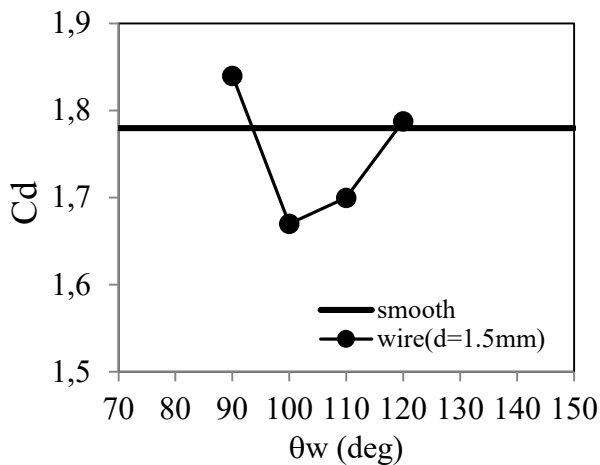
The pressure drag and the percentage of the pressure drag reduction for the two wires

configurations were shown in the table 1 and table 2 for Mach number 0.6 and 0.73. This shows that wires attached on the rear side of the cylinder significantly reduce the pressure drag compared to the smooth one. It should be also mentioned that the calculation of the drag did not taken into account the force acting on the wires. The percentage of the pressure drag reduction was not so high as in the case of using plates⁶⁾. It was 17% for Mach number 0.6 and 12% for Mach number 0.73, respectively.

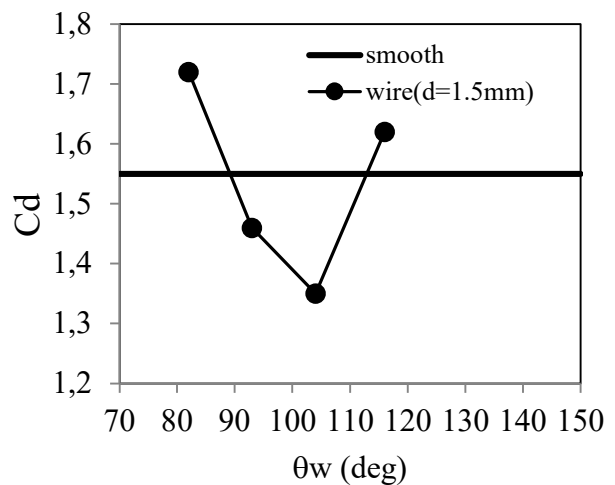
Table 1. Pressure drag coefficient

Mach Number	Double Wires d=1.5mm, $\theta_w = 110^\circ$		Four Wires (d=1.5mm)	
	Smooth	Wire	Smooth	Wire
0.6	1.557	1.34	1.557	1.32
		8		8

The pressure drag for different wire locations and wire diameter $d=1.5$ mm is plotted in figure 10 for both Mach number 0.6 and 0.73. It can be seen that the minimum drag was occurred $\theta_w = 110^\circ$ and $\theta_w = 100^\circ$ for both Mach



(a)



(b)

Figure 10. Pressure drag at different wire locations: (a) Mach number 0.6, (b) Mach number 0.73

0.73	1.779	1.70	1.779	1.71
		1		1

Table 2. Pressure drag reduction

Mach Number	Double Wires d=1.5mm, $\theta_w = 110^\circ$	Four Wires (d=1.5mm)
0.6	13.18%	14.50%
0.73	4.41%	4.07%

number 0.6 and 0.73, respectively. These results agreed with the results of the base pressure in section 3.1. This indicated that the maximum increasing of base pressure relates to the minimum pressure drag.

As for comparison, the effect of different wire diameters on the pressure drag was displayed in figure 11, where the pressure drag coefficient C_d was plotted against the wire diameter (d) for Mach number 0.6 and 0.73. The wire position was optimal to reduction pressure drag with similar to the location which have maximum base

pressure as can be seen in figure 5. It shows that wire configuration with the diameter 0.6 mm slightly decreased the pressure drag compared to smooth cylinder. This case was not so effective compared to others. For example, in the case of wire with the diameter 1 mm, and 1.5 mm the pressure drag was decreased much more.

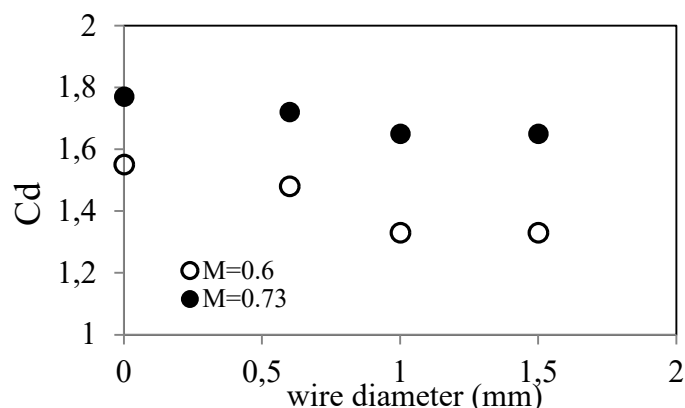


Figure 11. Effect of different wires diameter on pressure drag

4. Wires Effect on Wake Total

4.1. Wake Total Pressure

The presence of shock waves in the flow around the cylinder can increase the so-call wave drag. Therefore it was needed to effect. This measurement was based on the measurement of the total pressure wake behind the cylinder and the total drag, including the wave drag can be calculated from the wake total pressure. The

Pressure and Total Drag

additionally consider this phenomenon. The time-average pressure measurement used the rake, which was suggested to handle this rake was located at four cylinder diameters. This was assumed to be sufficient to capture the whole wake behind the cylinder.

The measurement was carried out with the wire diameter 1.5 mm

(double), for both Mach number 0.6 and 0.73. The wake total pressure distribution for this wire configuration was shown in figure 12, for both Mach number 0.6 and 0.73. It showed that the wire could increase the total pressure of the cylinder, compared to the smooth one. The

increasing of the total pressure taken by rake was similar to the increasing of pressure distribution of cylinder as mentioned in section 3.2. These results also showed that the existence of wires on the cylinder could reduce the wake size compared to the smooth cylinder.

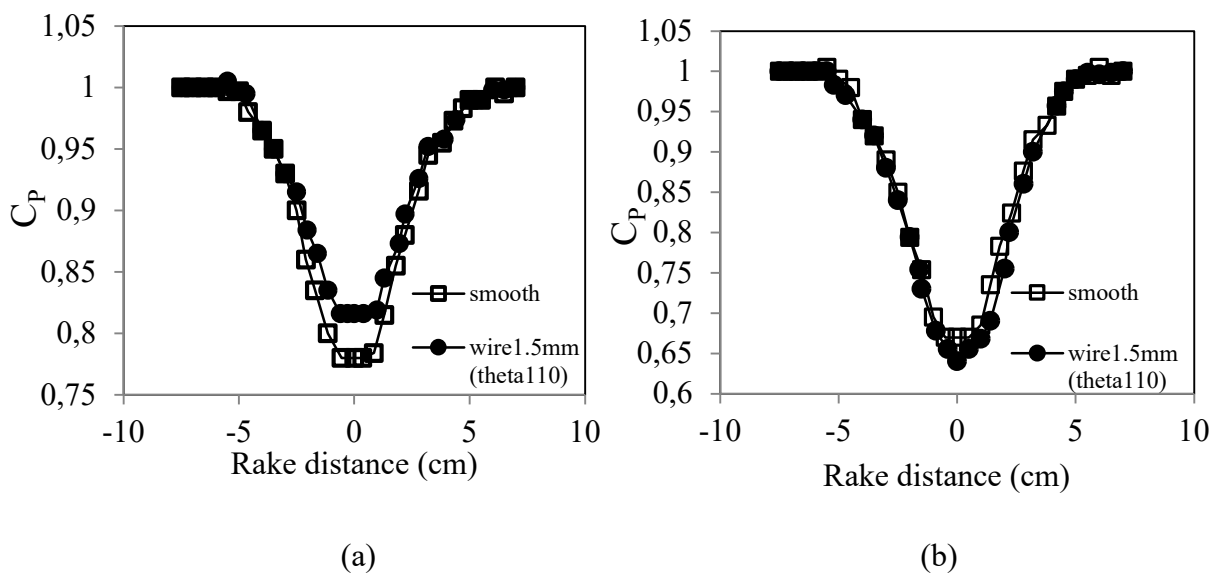


Figure 12. Effect of wires on wake total pressure distribution:
 (a) Mach number 0.6 ,(b) Mach number 0.73

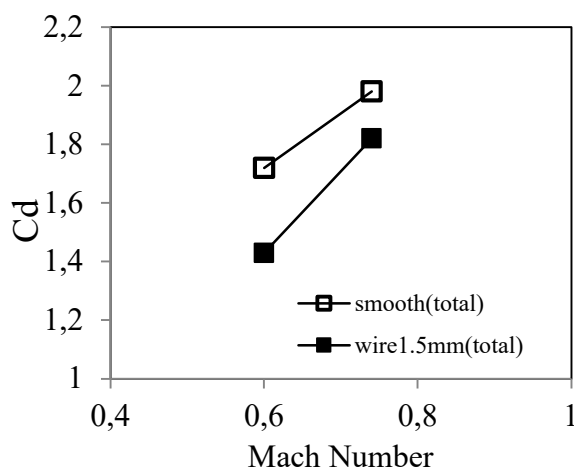
4.2. Total Drag

The total drag obtained in this experiment was calculated from the total-pressure distribution at rake^{7,8)}. The total drag coefficient for the symmetrical double-wire configuration is shown in figure 13, where the total drag coefficient C_{dt} was plotted against the Mach number. It was seen that the wire effect was to decrease the total drag, compared to the smooth cylinder. In this double-wire configuration, the

decreasing in the total drag was 16.6% for Mach number 0.6 and 8.3% for Mach number 0.73, respectively.

The comparison between the total drag coefficient and the pressure drag coefficient is shown in figure 14. This showed that the contribution of the pressure drag to the total drag was dominant. In the case of smooth cylinder the contribution of the pressure drag to

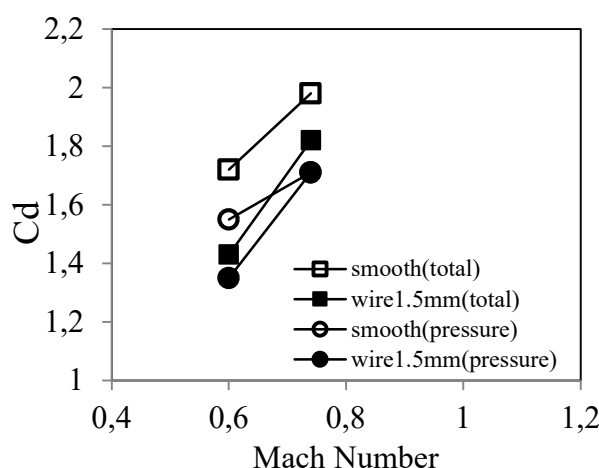
the total drag was 93% for Mach number 0.6 and 86.4% for Mach number 0.73, respectively. In the symmetrical double-wire



(a)

Figure 13. Effect of wires on total drag

configuration case, this contribution was 94% at Mach number 0.6 and 93.6% at Mach number 0.73, respectively.



(b)

Figure 14. Pressure drag contribution on total drag

5. Concluding remarks

In this experimental study, the influence of a passive control by using wire has been developed to reduce the drag for a circular cylinder at transonic speeds. Wires were arranged in the rear region of the cylinder so that the wires worked as barriers to restrict the upstream propagation of disturbances that originate in the near wake of the cylinder.

Based on the steady pressure measurement, it was observed that the wire could effectively increase the base pressure and the pressure behind the cylinder. This related to a

delay in the vortex formation, therefore the developed vortical pattern happened more downstream compared to the smooth cylinder case. So that depended on the Mach number, the wire effectively reduced the pressure drag by 13.2% for Mach number 0.6 and 4.4% for Mach number 0.73, respectively. Assuming the existence of shock waves that produce so-called wave drag, the wire also reduced the total drag: by 14% for Mach number 0.6 and 6% for Mach number 0.73.

By adding the wires numbers, i.e. changing the configuration from symmetrical double-wires to

symmetrical four-wires did not give any significant effect on the reduction of the pressure drag. In

Assuming the existence of strong shock waves at Mach number 0.73 caused the less effectiveness of wire in reducing the drag behind cylinder compared to the case of Mach number 0.6. Strong shock waves prevented disturbances to propagate upstream of the cylinder.

REFERENCES

- 1)Rodriguez, O., "The circular cylinder in subsonic and transonic flow," AIAA J. 22, 1713-1718 (1984).
- 2)Roshko, A., "On the wake and drag of bluff bodies," J. Aeronaut. Sci. 22, 124-132 (1955).
- 3) Bearman, P. W., "Investigation of the flow behind a two-dimensional model with a blunt trailing edge and fitted with splitter plates," J. Fluid Mech. 21, 241-255 (1965)
- 4)Achenbach, E. and Heinecke, E., "On vortex shedding from smooth and rough cylinders in the range of Reynolds numbers 6×10^3 to 5×10^5 ," J. Fluid Mech. 109, 239-251 (1981).
- 5)McCormick, Barnes W., *Aerodynamics, Aeronautics, and Flight Mechanics*, Jhon Willey & Sons, Inc., New York, 1979.
- 6)Thombi, L. and Nakamura, Y., "Suppression on flow separation on fact, only wires which are close to the free shear layer played a great role in this matter.
- a circular cylinder in transonic flow," Fluid Dynamic Symposium Japan, no 32, 251-254 (2000).
- 7)Schlichting, Hermann, *Boundary-Layer Theory*, 7th ed., translated by Dr. J. Kestin, McGraw-Hill Publishing Co., New York, 1979.
- 8)Kusunose, K., Crowder, J.P., and Watzlavick, R.L., "Wave drag extraction from profile drag based on a wake-integral method," AIAA 99-0275, January 1999.
- 9)Roshko, A., "Experiments on the flow past a circular cylinder at very high Reynolds number," J. Fluid Mech. 10, 345-356 (1961).
- 10)Batham. J. P., "Pressure distribution on circular cylinder at critical Reynolds numbers," J. Fluid Mech. 57, part2, 209-228 (1973).
- 11)Bearman. P. W., "On vortex shedding from a circular cylinder in the critical Reynolds number regime," J. Fluid Mech. 37, part3, 577-585 (1969).